

Effects of adaptive coupling on stochastic resonance of small-world networks

Dan Wu,^{*} Shiqun Zhu,[†] Xiaoqin Luo, and Liang Wu

School of Physical Science and Technology, Soochow University, Suzhou, Jiangsu 215006, People's Republic of China

(Received 22 January 2011; revised manuscript received 28 May 2011; published 2 August 2011)

The phenomenon of stochastic resonance in networks with small-world connectivity is investigated when the coupling strength is adaptive. The effects of the fixed and adaptive couplings on stochastic resonance of the system are discussed. It is found that the resonance is a monotonically increasing function of the adaptive coupling strength, while there is a peak when the coupling strength is fixed. The resonance for the adaptive coupling can reach a much larger value than that for fixed coupling.

DOI: [10.1103/PhysRevE.84.021102](https://doi.org/10.1103/PhysRevE.84.021102)

PACS number(s): 02.50.-r, 05.40.-a, 05.45.Xt

I. INTRODUCTION

During the past two decades, much attention has been devoted to the study of noise-induced constructive effects in nonlinear dynamical systems. For stochastic resonance, noise plays a constructive role in enhancing the detection and the transmission of a weak signal [1–5]. The investigation of stochastic resonance was extended to spatially extended systems. For example, Lindner *et al.* demonstrated that linear coupling, combined with noise and a weak periodic signal, can enhance the synchronization and the global organization in a chain of overdamped nonlinear oscillators, which is known as array-enhanced stochastic resonance [6]. Zhou *et al.* found array-enhanced coherence resonance [7] in an array of coupled FitzHugh-Nagumo neurons.

Subsequently, the study of the dynamics of spatially extended systems of regular coupled networks [8,9] was extended to networks with complex topologies such as small-world [10,11] and scale-free networks [12,13]. In particular, the effects of coupling on stochastic resonance in complex networks were explored. For example, the stochastic resonance on the excitable Watts-Strogatz small-world network was studied by means of the discrete Rulkov map. It was shown that the small-world property was able to enhance the stochastic resonance only for intermediate coupling [14]. Moreover, the phenomenon of stochastic resonance was explored in locally paced scale-free networks of bistable oscillations, where an optimal coupling strength was needed for the best noise-induced global response [15,16].

However, most of the previous studies were devoted to the fixed coupling cases. In considering the spontaneity of self-organizing complex systems, it is natural that the suitable coupling strength can be adaptive [17–21]. In many realistic systems such as neuronal networks and biological systems [22,23], networks with an adaptively changed coupling may be more reasonable. Meanwhile, the evolution of the network connectivity has also been found in social [24,25], ecological [26], and epidemic networks [27], where agents or specials learn from the state of the networks and adapt their behaviors accordingly. For example, in neural systems, the coupling enhances for synchronized oscillators and weakens for non-synchronized pairs, which is known as the Hebbian learning rules [22] and is helpful in the understanding of the mechanism

of learning and memory of the brain [28]. The synchronization of coupled oscillator networks was investigated when the adaptive coupling, also called time-varying coupling, was included in the system [29]. Different from the Hebbian learning rule of adaptive coupling, the adaptive scheme can be designed in such a way that the coupling grows stronger for the pair of oscillators that has a larger difference [29]. For example, to achieve consensus on some opinion, agents try to approach those individuals who have opinions that are different from their own and persuade them to follow their common opinion, while they do not have to put much effort into enhancing the interaction with others already sharing similar opinions [30]. For adaptive coupling, the coupling strength between two oscillators is increased with its changing rate related to the difference between the dynamical behaviors of the oscillators involved. It is found that the synchronization is improved by the adaptive coupling, that is, the adaptive coupling is more efficient for the onset of synchronization in networks as compared with the case of fixed coupling. However, the impact of the adaptive coupling on stochastic resonance needs to be studied further.

In this paper the phenomenon of stochastic resonance in networks with small-world connectivity is investigated when the coupling strength is adaptive [29]. Since the dynamical behavior is highly sensitive to the coupling factor in the context of periodically forced coupled oscillators, it is pertinent to compare the effects of the fixed and the adaptive couplings on the stochastic resonance. In Sec. II the dynamical model of the coupled bistable system with small-world connectivity is presented. The effects of the small-world feature and noise on the average adaptive coupling are discussed. In Sec. III the effects of the small-world topology and the controlling parameter of the adaptive coupling on the resonant response are investigated. In Sec. IV a comparison between the fixed and the adaptive couplings on stochastic resonance is presented. The synchronization of the complex network is analyzed by comparing the two coupling cases.

II. DYNAMICAL MODEL

An ensemble of N coupled bistable elements with small-world topologies can be written as

$$\begin{aligned} \dot{x}_i(t) = & x_i(t) - x_i^3(t) + \sqrt{2\sigma}\xi_i(t) + A \sin(\Omega t) \\ & + \frac{1}{k_i} \sum_{j=1}^N c_{ij}(t)[x_j(t) - x_i(t)], \end{aligned} \quad (1)$$

^{*}wud@suda.edu.cn

[†]szhu@suda.edu.cn

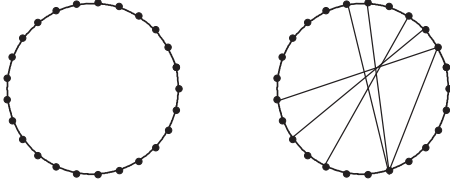


FIG. 1. Examples of considered network topologies. (a) Regular ring characterized by $p = 0$ with periodic boundary conditions. (b) The Newman-Watts small-world topology is constructed by randomly adding links between two originally separate elements.

where σ is the intensity of the Gaussian thermal noise $\xi_i(t)$ with $\langle \xi_i(t) \rangle = 0$ and $\langle \xi_i(t) \xi_j(t') \rangle = \delta_{ij} \delta(t - t')$, A is the amplitude of the external periodic signal, and $\Omega = 2\pi/T$ is the frequency of the signal. The variable $x_i(t)$ ($i = 1, \dots, N$) is the position of the i th element at time t and N is the number of elements in the network. The network with Newman-Watts small-world topologies [11] is constructed by randomly adding connectivity on an originally regular network in which each element is connected only with its nearest neighbors. The probability that a new link is added between two originally separate elements is p . The total number of possible shortcuts is $\frac{N(N-1)}{2}$. If there are n_e shortcuts added, the probability is $p = \frac{2n_e}{N(N-1)}$. Therefore, p is a normalized shortcut number added in the network. When $p = 0$, the network is a nearest-neighbor coupled network. While a globally coupled network is constructed, $p = 1$. For $0 < p < 1$, the constructed network shows small-world features. The degree k_i of element i is the number of its neighbors. Typical examples of network topologies are shown in Fig. 1. For clarity, only 25 vertices are displayed in each panel. The regular ring is plotted in Fig. 1(a). Each vertex is connected to its $k = 2$ nearest neighbors. The Newman-Watts small-world topology is shown in Fig. 1(b) when links are randomly added between two originally separate elements. In Fig. 1(b), $n_e = 6$ shortcuts are added. The probability is $p = \frac{2n_e}{N(N-1)} = 0.02$.

When adaptive coupling [29] is applied, the coupling strength between nodes i and j can be defined as

$$\dot{c}_{ij}(t) = \dot{c}_{ji}(t) = \lambda [x_j(t) - x_i(t)]^2, \quad (2)$$

where the overdot denotes differentiation with respect to time t . The adaptive coupling c_{ij} at time t increases at a changing rate related to the difference of the behavior between elements i and j . The coupling strength increases proportionally to the synchronization difference in order to suppress the difference. This is understandable in social and economical networks, where agents learn from the state of the elements and adapt their behaviors accordingly for common opinions or interests [18,30]. The non-negative parameter λ controls the growth speed of the coupling strength. If the noise σ between the elements is varied, the difference between elements i and j changes correspondingly. If the normalized shortcut number p is varied, the behavior between the two elements also changes accordingly, that is, the adaptive coupling is a combined function of σ , λ , and p .

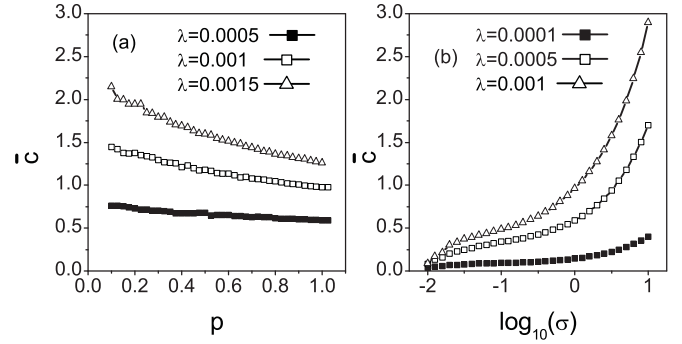


FIG. 2. Average coupling \bar{c} as a function of the normalized shortcut p and the noise strength σ for different values of the controlling parameter λ . The parameters are $N = 500$, $T = 10^3$, $A = 0.2$, and $u_0 = 0.454$. (a) \bar{c} as a function of p with $\sigma = 1$. (b) \bar{c} as a function of σ with $p = 1$.

By averaging Eq. (2) over the whole population and time, the average adaptive coupling \bar{c} can be written as

$$\bar{c} = \lim_{T \rightarrow \infty} \frac{1}{N^2 T} \sum_{i=1}^T \sum_{i=1}^N \sum_{j=1}^N c_{ij}(t). \quad (3)$$

The average adaptive coupling strength \bar{c} is illustrated in Fig. 2 as a function of the normalized shortcut number p and the noise strength σ for different values of λ . The average adaptive coupling strength \bar{c} is plotted in Fig. 2(a) as a function of p when λ is varied. It is found that the average coupling strength \bar{c} is a monotonically decreasing function of p . If more edges are added, each element has more (but not necessarily nearest) neighbors by increasing normalized shortcut number p . For the system it is easy to reach synchronization with increasing p . Therefore, the difference between elements i and j is reduced. The average adaptive coupling depending on the evolution of Eq. (2) is correspondingly reduced. The average adaptive coupling strength \bar{c} is plotted in Fig. 2(b) as a function of σ when λ is varied. It is seen that \bar{c} increases with increasing σ , that is, the increasing noise enhances the difference between elements i and j . This leads to a monotonic increase of the average adaptive coupling. From Fig. 2 it is clear that the average coupling \bar{c} increases as the controlling parameter λ increases. This is understandable from the evolution equation [Eq. (2)] of the adaptive coupling.

III. EFFECTS OF ADAPTIVE COUPLING ON STOCHASTIC RESONANCE

To investigate the response of the periodically driven system, the spectral amplification factor $\eta = 4A^{-2} |\langle e^{i\Omega t} X(t) \rangle|^2$ is calculated [31], where $X(t) = \frac{1}{N} \sum_{i=1}^N x_i(t)$ is the average position of the elements at time t . The spectral amplification factor η can provide a precise amount of information in the signal transported with a particular forcing period. It can be used as a numerically effective measure for stochastic resonance.

The spectral amplification factor η as a function of the controlling parameter λ , the noise strength σ , and the normalized shortcut number p is shown in Fig. 3. The spectral amplification factor η is plotted in Fig. 3(a) as a function of σ

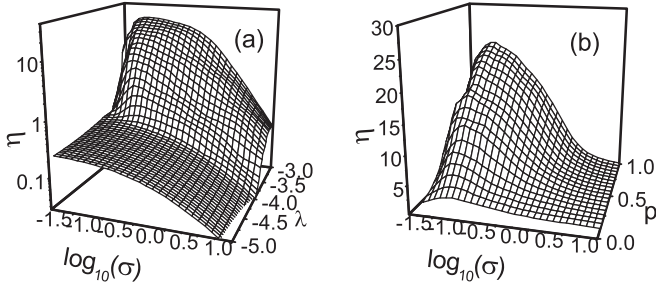


FIG. 3. Three-dimensional plot of the spectral amplification factor η as a function of the noise strength σ , the controlling parameter λ , and the normalized shortcut number p . The parameters are $N = 500$, $T = 10^3$, $A = 0.2$, and $u_0 = 0.454$. (a) η as a function of σ and λ with $p = 1$. (b) η as a function of σ and p with $\lambda = 0.001$.

and λ . For small λ , the spectral amplification factor decreases monotonically as the noise strength increases. For large λ , there exists an optimal value of the noise intensity for which the resonance is maximum. This is the characteristic signature of stochastic resonance. The maximum of the resonance increases as the controlling parameter λ increases. This mechanism can be explained as follows. The increase of the controlling parameter λ means the increase of the average adaptive coupling as shown in Fig. 2. There is an enhancement of the connection between elements. When an element overcomes the potential barrier with the help of external forcing, the increasing coupling between elements can help the excited element pull some of the coupled neighbors to respond to external signals. This causes an enhancement of the resonance. The spectral amplification factor η is plotted in Fig. 3(b) as a function of σ and p . It is found that the resonance is enhanced as the normalized shortcut number p between elements increases. This is understandable since the increase of p means more edges are added between two originally separate elements. The increased connection between elements may help mutual excitation and lead to an enhancement of the stochastic resonance.

The spectral amplification factor η as a function of the average adaptive coupling strength \bar{c} is plotted in Fig. 4 for different values of the noise strength σ and the normalized shortcut number p . The average adaptive coupling strength

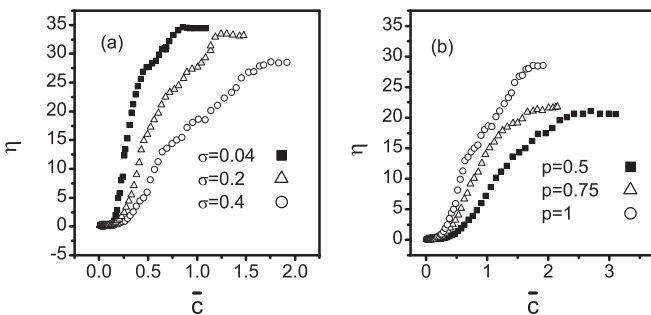


FIG. 4. Spectral amplification factor η as a function of the average coupling strength \bar{c} . The parameters are $N = 500$, $T = 10^3$, $A = 0.2$, and $u_0 = 0.454$. (a) η as a function of \bar{c} for different values of the noise strength σ with $p = 1$. (b) η as a function of \bar{c} for different values of the normalized shortcut number p with $\sigma = 0.4$.

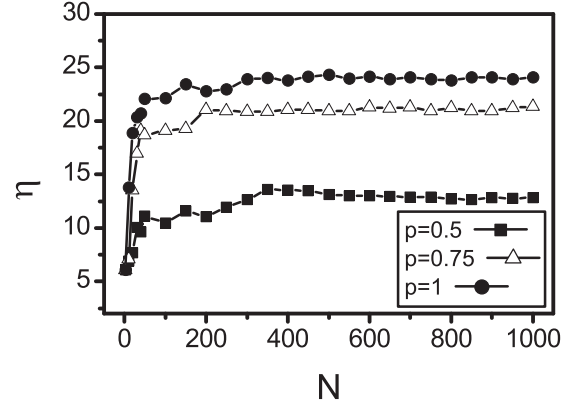


FIG. 5. Spectral amplification factor η as a function of the particle number N for different values of the normalized shortcut number p . The parameters are $T = 10^3$, $A = 0.2$, $u_0 = 0.454$, $\sigma = 0.04$, and $\lambda = 0.001$.

\bar{c} obtained from Eq. (3) is varied by varying the controlling parameter λ from $\lambda = 10^{-5}$ to 10^{-2} . The spectral amplification factor η is plotted in Fig. 4(a) as a function of \bar{c} for different values of noise strength σ . The value of η decreases as σ increases while η increases as \bar{c} increases, that is, the larger the noise disturbance is, the smaller the resonance becomes. The spectral amplification factor η is plotted in Fig. 4(b) as a function of \bar{c} for different values of the normalized shortcut number p . The value of η increases as p and \bar{c} increase, that is, the larger the normalized shortcut number p is, the larger the resonance becomes. The resonance of the system increases and finally saturates to a constant as the average adaptive coupling increases.

To see the response of the system that is dependent on the system size, the spectral amplification factor η as a function of the particle numbers N is plotted in Fig. 5. It is clear that η is almost a constant for sufficiently large numbers with $N > 300$ while for small numbers η increases very fast as N increases from zero. The phenomenon of system-size resonance [32] does not appear since the system-size resonance could only appear in the case of subthreshold dynamics, where the driving force alone is unable to provoke jumps between elements. However, for large amplitudes of the forcing $A = 0.2$ in this paper, the response grows monotonically with N and finally saturates to finite values [33,34].

IV. FIXED AND VARYING COUPLINGS

For fixed coupling, the coupling between the two elements i and j is c_{ij} . If the two elements are coupled to each other, the coupling is $c_{ij} = c_{ji} = C$; otherwise $c_{ij} = 0$. The ensemble of N coupled bistable elements with the fixed coupling strength can be written as

$$\dot{x}_i(t) = x_i(t) - x_i^3(t) + \sqrt{2}\sigma\xi_i(t) + A \sin(\Omega t) + \frac{1}{N-1} \sum_{j=1}^N C[x_j(t) - x_i(t)]. \quad (4)$$

For simplicity, the globally coupled case of $p = 1$ is considered. The approximate theory [29] can be applied.

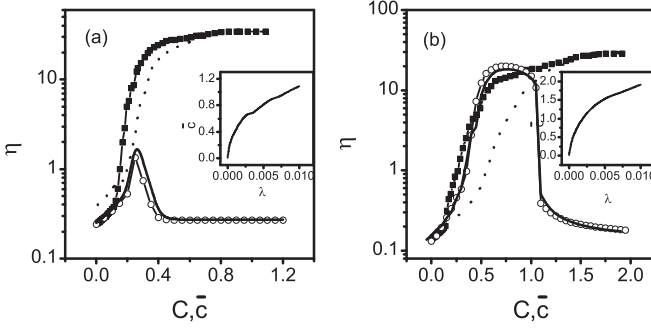


FIG. 6. Spectral amplification factor η as a function of the fixed coupling strength C (circles) and the average coupling strength \bar{c} (squares). The parameters are $N = 500$, $T = 10^3$, $A = 0.2$, $p = 1$, and $u_0 = 0.454$. The solid line shows the theoretical predictions of Eq. (6) and the dotted line shows the theoretical predictions of Eqs. (7) and (8). (a) $\sigma = 0.04$. (b) $\sigma = 0.4$.

By introducing the average position of the units, $X(t) = \frac{1}{N} \sum_{i=1}^N x_i(t)$, and averaging Eq. (4) over the whole population with periodic boundary condition, one has

$$\dot{X}(t) = X(t) - \frac{1}{N} \sum_i x_i^3(t) + A \sin(\Omega t). \quad (5)$$

When $x_i = X + \delta_i$ and $\frac{1}{N} \sum_i \delta_i^2 = M$ is introduced, Eq. (5) can be written as

$$\dot{X}(t) = [1 - 3M(t)]X(t) - X^3(t) + A \sin(\Omega t), \quad (6)$$

where the variation of the second moment $M(t)$ can be calculated by numerically solving Eq. (6). The spectral amplification factor η of the coupled bistable system is plotted in Fig. 6 as a function of the fixed coupling strength C . Circles correspond to numerical simulations from a direct integration of Eq. (4). The lines are the corresponding theoretical predictions of Eq. (6). It is found that the theoretical predictions of Eq. (6) are in good agreement with the results from direct numerical simulations of Eq. (4).

The spectral amplification factor η of the coupled bistable system as a function of the fixed coupling strength C and the average coupling strength \bar{c} is plotted in Fig. 6. The average coupling strength \bar{c} is obtained by varying the parameter λ from 10^{-5} to 10^{-2} , as shown in the inset. Circles correspond to the stochastic resonance for fixed coupling while squares correspond to that for adaptive coupling. The spectral amplification factor η is plotted in Fig. 6(a) as a function of C and \bar{c} for small noise strength $\sigma = 0.04$. For small noise strength the spectral amplification factor η for the adaptive coupling case reaches a larger value compared to that for the fixed coupling. The spectral amplification factor η increases as the average coupling strength \bar{c} increases and almost saturates as \bar{c} increases further. For fixed coupling there is a peak in η with an optimal value of C . These phenomena can be explained by the different mechanisms of the connections between elements caused by the adaptive coupling and the fixed coupling. In the case of adaptive coupling, when one element (referred to as node O) is able to overcome the potential barrier with the help of external forcing, its neighbor

increases its coupling with node O . The greater the difference is between node O and its coupled neighbor, the stronger the corresponding coupling is. It may dramatically change the dynamical behavior of the neighbors coupled with node O . Thus it may raise corresponding couplings at the next time step and finally drive the neighbors to be synchronized with node O . Meanwhile, if the difference between node O and its neighbors is small, only small adaptive coupling is needed. Since the connections in the complex network are correlated with each other, the mechanism of adaptive coupling may excite more elements when the average adaptive coupling strength equals the fixed coupling strength. Therefore, the resonance for the adaptive coupling is larger than that the fixed coupling case. The increase of the time-varying coupling can continuously excite more and more elements to respond to the external signal and thus a continuous increase in η . For fixed coupling, when node O overcomes the potential barrier with the help of external forcing, the fixed coupling between elements can help node O pull some of the coupled neighbors and produce a collective, macroscopic movement. However, the number of elements excited by the fixed coupling may saturate to a finite value even if the fixed coupling is large enough. The further increase of the fixed coupling can simply reinforce the synchronization of the excited elements. The typical effect of array-enhanced resonance disappears for a sufficiently large value of the fixed coupling [6,7]. As a result, the resonance is a nonmonotonic function of the fixed coupling strength.

The spectral amplification factor η is plotted in Fig. 6(b) as a function of C and \bar{c} for large noise strength $\sigma = 0.4$. For large noise strength the spectral amplification factor η increases and finally reaches a constant value, which is a bit smaller than that for the small noise case [Fig. 6(a)] when the average adaptive coupling \bar{c} increases. It seems that the adaptive coupling can always adjust the connection between elements to efficiently respond to the external signals, while for fixed coupling there exists an optimal value of C for which η is maximum. The maximum of η is much higher than that for the small noise case [Fig. 6(a)]. This is understandable since the increase of the noise disturbance enhances the number of elements that are excited by the fixed coupling and leads to an increase in the maximum of the spectral amplification factor. However, even with the help of noise, the number of elements excited by fixed coupling is still smaller than the number excited by adaptive coupling. Therefore, the maximum of η for the fixed coupling case is always smaller than the maximum of η for adaptive coupling regardless of the values of the noise strength. Notably, the optimal value of the fixed coupling strength for the maximum of the resonance has been reported in Ref. [35]. In that case, increasing the fixed coupling can excite only a finite number of elements while increasing the adaptive coupling can excite more and more elements to respond to the external signal.

For varying couplings it is difficult to develop a general analytical method for the model of Eq. (1) due to the complexity of the small-world network. However, when the system is globally coupled with $k_i = N - 1$ and $p = 1$, the approximate theory can be applied [32]. In the approximation one can write $x_i = X + \delta_i$ and assume that δ_i is an independent Gaussian random variable with zero mean

and variance M . By assuming that $N^{-1} \sum_i \delta_i^2 = M$ and $c_{ij}(t) = \bar{c} + \Delta_{ij}$, Eq. (1) can be rewritten as

$$\dot{X}(t) = X(t) - X^3(t) - 3MX(t) + \sqrt{\frac{2\sigma}{N}} \xi(t) + A \sin(\Omega t), \quad (7)$$

$$\frac{1}{2} \dot{M} = M - 3X^2M - 3M^2 - \frac{N}{N-1} \bar{c}M - \frac{1}{N(N-1)} M' + \sigma, \quad (8)$$

where $\xi(t)$ is the Gaussian white noise with $\langle \xi(t) \rangle = 0$ and $\langle \xi_i(t) \xi_j(t') \rangle = \delta_{ij} \delta(t - t')$. In the limit $N \rightarrow \infty$, the noise term ξ vanishes. The parameter $M' = \sum_{i=1}^N \delta_i^2 \sum_{j=1}^N \Delta_{ij}$ can be determined by the combined numerical simulations of Eqs. (1), (7), and (8), where Δ_{ij} is the deviation of $c_{ij}(t)$ from the average coupling strength \bar{c} . The spectral amplification factor η of the coupled bistable system is plotted in Fig. 6 as a function of the average coupling strength \bar{c} . Squares correspond to numerical simulations from a direct integration of Eq. (1) and dotted lines are the corresponding theoretical predictions of Eqs. (7) and (8). Though there are noticeable discrepancies in η , reasonably good agreement is obtained.

The contour plot of the spectral amplification factor η as a function of the noise strength σ and the fixed coupling strength C is plotted in Fig. 7. There exists an optimal value of σ , which is the characteristic signature of stochastic resonance. There also exists an optimal coupling strength C , which is the main result of array-enhanced stochastic resonance [6]. The squares mark the optimal values of the coupling strength C for different values of σ . It is found that the peak position of η is shifted to a large value of the coupling strength C when σ is increased. The mechanism can be understood as follows. When the coupling C between elements is increased, an element may be excited by its neighboring elements even though it may be unable to respond to the external stimulus. As a whole, the coherence of the motion in the coupled system is enhanced by mutual excitation. However, if the coupling is too strong, the excited elements may become synchronized and behave as a

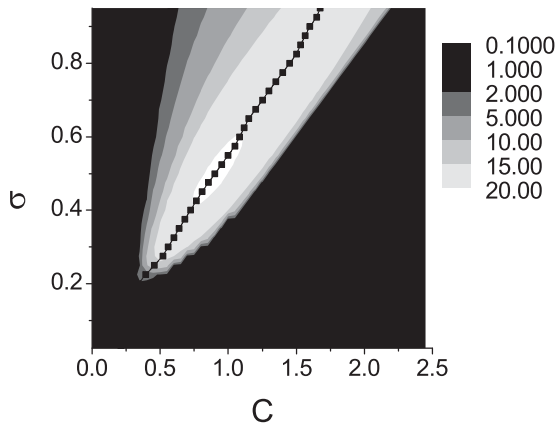


FIG. 7. Contour plot of the spectral amplification factor η as a function of the noise strength σ and the fixed coupling strength C . Each square marks the optimal C for a given noise strength σ . The parameters are $N = 500$, $T = 10^3$, $A = 0.2$, and $u_0 = 0.454$.

single element. The typical effect of array-enhanced resonance disappears [6,7]. For a noise disturbance that is too large, some of the elements pulled by noise offer too much resistance to follow the external force. A greater coupling strength is needed for the favorable elements to overcome the resistant effects. Therefore, the optimal value of η is shifted to a large value of the coupling strength C when the noise strength σ is increased.

It is seen in Fig. 7 that the peak in the spectral amplification factor η appears around the optimal values of the noise strength σ and the coupling strength C . When the noise strength $\sigma = 0.04$, the peak in η appears around $C = 0.23$; when $\sigma = 0.4$, the peak appears around $C = 0.75$. This is consistent with the plot shown in Fig. 6.

To provide a better understanding of the results presented, the synchronization of the complex network is investigated. The synchronization behavior can be expressed by the mean square deviation [35–37]

$$\gamma^2 = \frac{1}{N} \left\langle \sum_{i=1}^N [x_i(t) - \langle x \rangle]^2 \right\rangle_t, \quad (9)$$

where $\langle x \rangle$ denotes the average over the elements of the array, $\langle x \rangle = \frac{1}{N} \sum_{i=1}^N x_i(t)$, and $\langle \cdot \cdot \cdot \rangle_t$ denotes the average over time. A large value of γ represents large deviations between various oscillators and a small value of γ denotes strong collective motion and, consequently, better synchronization [35–37].

The mean square deviation γ is plotted in Fig. 8 as a function of the fixed coupling strength C and the average adaptive coupling strength \bar{c} . The average adaptive coupling \bar{c} is obtained by varying the controlling parameter λ from 10^{-5} to 10^{-2} . The weak noise of $\sigma = 0.04$ and the strong noise $\sigma = 0.4$ are plotted in Figs. 8(a) and 8(b), respectively. It is found that γ decreases when either C or \bar{c} increases, that is, both the fixed coupling and the adaptive coupling can improve the synchronization of the system. The synchronization of the whole system for adaptive coupling is always better than that for fixed coupling. This is because the increase of the adaptive coupling can continuously excite more and more neighbors to be synchronized with the excited node O , as illustrated in Fig. 6. The larger the difference between node O and its neighbors, the stronger the adaptive coupling is. In contrast, if the difference between node O and its neighbor is small, only a small value of the adaptive coupling is needed. Therefore,

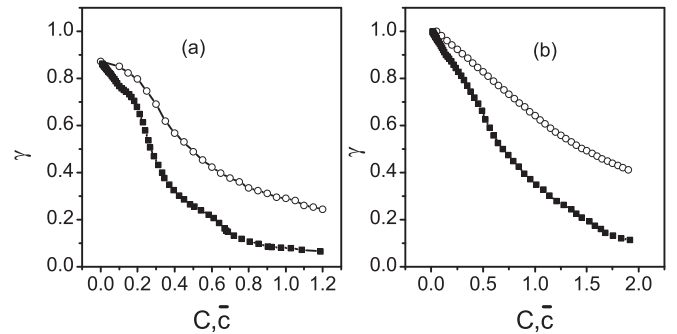


FIG. 8. Variance γ plotted as a function of the fixed coupling strength C (circles) and the average coupling strength \bar{c} (squares). The parameters are $N = 500$, $T = 10^3$, $A = 0.2$, $p = 1$, and $u_0 = 0.454$. (a) $\sigma = 0.04$. (b) $\sigma = 0.4$.

the elements can reach good synchronization with a small amount of average adaptive coupling. As the connections in the complex network are correlated with each other, the synchronization of the whole system can be greatly enhanced with an increase of the average adaptive coupling \bar{c} ; however, for fixed coupling, increasing C can only reinforce the global synchronization between the excited elements. Since there always exists a small number of elements that cannot be excited by the fixed coupling, as illustrated in Fig. 6, the synchronization of the whole system is poor compared with that of adaptive coupling.

V. DISCUSSION

The phenomenon of stochastic resonance in networks with small-world connectivity is investigated when the coupling strength is varied at a changing rate related to the difference of the behavior between elements. It is found that the resonance is a monotonically increasing function of the adaptive coupling strength, while there is a peak for the fixed coupling strength. The resonance for the adaptive coupling can reach a much larger value. This may be explained by the different mechanisms of connections between elements caused by

the adaptive coupling and the fixed coupling. The adaptive coupling can excite more and more elements to respond to external signals, while the elements excited by the fixed coupling may reach a finite number. The further increase of the fixed coupling strength can only reinforce the global synchronization between the excited elements. Moreover, the synchronization of the whole system for the adaptive coupling is better than that for the fixed coupling, which agrees with the previous results reported in Ref. [29]. Due to the importance of the adaptive coupling in various networks, such as neuronal networks [22], biological systems [23], social networks [24,25,30], ecological networks [26], and epidemic networks [27], it is expected that the present study can be applied in realistic experiments and foster the understanding of the processes in which adaptive coupling plays a major role [38–40].

ACKNOWLEDGMENTS

Financial support from the National Natural Science Foundation of China (Grants No. 11005077 and No. 10847156) and the Pre-research Project of Soochow University are gratefully acknowledged.

-
- [1] J. Dougllass, L. Wilkens, E. Pantazelou, and F. Moss, *Nature (London)* **365**, 337 (1993).
 - [2] K. Wiesenfeld and F. Moss, *Nature (London)* **373**, 33 (1995).
 - [3] P. Jung, *Phys. Rep.* **234**, 175 (1993).
 - [4] L. Gammaitoni, P. Hänggi, P. Jung, and F. Marchesoni, *Rev. Mod. Phys.* **70**, 223 (1998).
 - [5] A. A. Zaikin, J. Kurths, and L. Schimansky-Geier, *Phys. Rev. Lett.* **85**, 227 (2000).
 - [6] J. F. Lindner, B. K. Meadows, W. L. Ditto, M. E. Inchiosa, and A. R. Bulsara, *Phys. Rev. Lett.* **75**, 3 (1995).
 - [7] C. Zhou, J. Kurths, and B. Hu, *Phys. Rev. Lett.* **87**, 098101 (2001).
 - [8] R. Albert and A.-L. Barabasi, *Rev. Mod. Phys.* **74**, 47 (2002).
 - [9] S. Boccaletti, V. Latora, Y. Moreno, M. Chavez, and D.-U. Hwang, *Phys. Rep.* **424**, 175 (2006).
 - [10] D. J. Watts and S. H. Strogatz, *Nature (London)* **393**, 440 (1998).
 - [11] M. E. J. Newman and D. J. Watts, *Phys. Lett. A* **263**, 341 (1999).
 - [12] A.-L. Barabasi and R. Albert, *Science* **286**, 509 (1999).
 - [13] L. Wu, S. Zhu, and X. Luo, *Chaos* **20**, 033113 (2010).
 - [14] M. Perc, *Phys. Rev. E* **76**, 066203 (2007).
 - [15] M. Perc and M. Gosak, *New J. Phys.* **10**, 053008 (2008).
 - [16] M. Perc, *Phys. Rev. E* **78**, 036105 (2008).
 - [17] Y.-C. Lai, M. G. Frei, and I. Osorio, *Phys. Rev. E* **73**, 026214 (2006).
 - [18] Q. Ren and J. Zhao, *Phys. Rev. E* **76**, 016207 (2007).
 - [19] D. Huang, *Phys. Rev. E* **69**, 067201 (2004).
 - [20] H. Leung and Z. Zhu, *Phys. Rev. E* **69**, 026201 (2004).
 - [21] S. Boccaletti, D.-U. Hwang, M. Chavez, A. Amann, J. Kurths, and L. M. Pecora, *Phys. Rev. E* **74**, 016102 (2006).
 - [22] J. Ito and K. Kaneko, *Phys. Rev. Lett.* **88**, 028701 (2001).
 - [23] M. Chavez, M. Valencia, V. Navarro, V. Latora, and J. Martinerie, *Phys. Rev. Lett.* **104**, 118701 (2010).
 - [24] B. Skyrms and R. Pemantle, *Proc. Natl. Acad. Sci. USA* **97**, 9340 (2000).
 - [25] A. W. Lo, *J. Portfolio Manage.* **30**, 15 (2004).
 - [26] U. Dieckmann and M. Doebeli, *Nature (London)* **400**, 354 (1999).
 - [27] T. Gross, Carlos J. Dommar D’Lima, and B. Blasius, *Phys. Rev. Lett.* **96**, 208701 (2006).
 - [28] P. Seliger, S. C. Young, and L. S. Tsimring, *Phys. Rev. E* **65**, 041906 (2002).
 - [29] D. Huang, *Phys. Rev. E* **74**, 046208 (2006).
 - [30] J.-F. Zhu, M. Zhao, W. Yu, C. Zhou, and B.-H. Wang, *Phys. Rev. E* **81**, 026201 (2010).
 - [31] C. J. Tessone, C. R. Mirasso, R. Toral, and J. D. Gunton, *Phys. Rev. Lett.* **97**, 194101 (2006).
 - [32] A. Pikovsky, A. Zaikin, and M. A. de la Casa, *Phys. Rev. Lett.* **88**, 050601 (2002).
 - [33] D. Cubero, *Phys. Rev. E* **77**, 021112 (2008).
 - [34] M. Morillo, J. G. Ordóñez, and J. M. Casado, *Eur. Phys. J. B* **74**, 211 (2010).
 - [35] Z. Gao, B. Hu, and G. Hu, *Phys. Rev. E* **65**, 016209 (2001).
 - [36] C. Masoller and A. C. Marti, *Phys. Rev. Lett.* **94**, 134102 (2005).
 - [37] Q. Wang, Z. Duan, M. Perc, and G. Chen, *Europhys. Lett.* **83**, 50008 (2008).
 - [38] B. Ravoori, A. B. Cohen, A. V. Setty, F. Sorrentino, T. E. Murphy, E. Ott, and R. Roy, *Phys. Rev. E* **80**, 056205 (2009).
 - [39] F. Sorrentino, *Phys. Rev. E* **80**, 056206 (2009).
 - [40] R. Chacon and L. Marcheggiani, *Phys. Rev. E* **82**, 016201 (2010).